Shell-model description of magnetic dipole bands in ^{105}Sn

M. Honma,[*1] T. Otsuka,[*2,*3,*4,*5] T. Mizusaki,[*6] Y. Utsuno,[*7,*8] N. Shimizu,[*8] and M. Hjorth-Jensen[*4,*9,*10]

Because of the well-developed shell closure at N, $Z = 50$, Sn isotopes have often been studied using the shell model by considering only valence neutrons. However, several states have been observed in light Sn isotopes that would be described by the configurations with a broken ^{100}Sn core. One interesting example is the high-spin regular band that decays mainly by M1 transitions.[1)] This band has been interpreted by the "shears mechanism" using the tilted-axis cranking model.[2)] In this report, we present the results of our trial to describe this magnetic dipole band using the shell model, taking ^{105}Sn as an example.

The adopted model space consists of the proton ($0g_{9/2}$, $1d_{5/2}$, $0g_{7/2}$) orbits and the neutron ($1d_{5/2}$, $0g_{7/2}$, $0h_{11/2}$, $2s_{1/2}$, $1d_{3/2}$) orbits. The effective interaction is prepared by combining the SNBG1[3)] interaction as neutron-neutron and proton-proton part, the P1GD5G3[4)] interaction for proton-neutron part among the relevant orbits if defined, and for the rest parts the microscopic interaction[5)] based on the realistic N^{3}LO interaction.[6)] The bare single-particle energies (SPEs) for the neutron orbits are adjusted so as to reproduce the effective SPEs obtained by the SNBG1 interaction at ^{114}Sn. The SPE of the proton $0g_{9/2}$ orbit is taken from the P1GD5G3 interaction, and the rest are determined so that the effective SPEs agree with those of the neutrons at ^{100}Sn. In order to ensure the computational feasibility, up to 5 nucleons are allowed to excite into the proton ($1d_{5/2}$, $0g_{7/2}$) orbits or neutron ($0h_{11/2}$, $2s_{1/2}$, $1d_{3/2}$) orbits.

The calculated band structure is shown in Fig. 1. One can find reasonable agreement between the experimental data and the shell-model results. The E2 and M1 transition probabilities are calculated by using the effective charge $e_p = 1.6$, $e_n = 0.8$, and the effective spin g-factors $g^{\mathrm{eff}} = 0.74g^{\mathrm{free}}$. The calculated negative parity band $43/2^-_1$-$41/2^-_1$-$39/2^-_1$-$\cdots$ decays mainly by M1 transitions, consistently with the experiment. The typical $B(M1)$ value within the band is $\sim 1\mu_N^2$, while the $B(E2)$ value is at most $0.08\mathrm{e}^2\mathrm{b}^2$, indicating the M1 dominance. In addition to this band, the shell-model results give a positive-parity M1-dominant band $39/2^+_2$-$37/2^+_3$-$35/2^+_2$-$\cdots$, on top of the $23/2^+_2$ state. The dominant configurations in the calculated wave functions are $\pi(g_{9/2})^{-1}(g_{7/2})^1\nu(g_{7/2}d_{5/2})^4(h_{11/2})^1$ and $\pi(g_{9/2})^{-1}(g_{7/2})^1\nu(g_{7/2}d_{5/2})^5$ relative to the ^{100}Sn closed core for the negative and the positive parity bands, respectively. However, the purity of these configurations is gradually lost for lower spin states, and the feature of the "shears mechanism," *i.e.*, a rapid decrease of $B(M1)$ with increasing spin, is not clear.

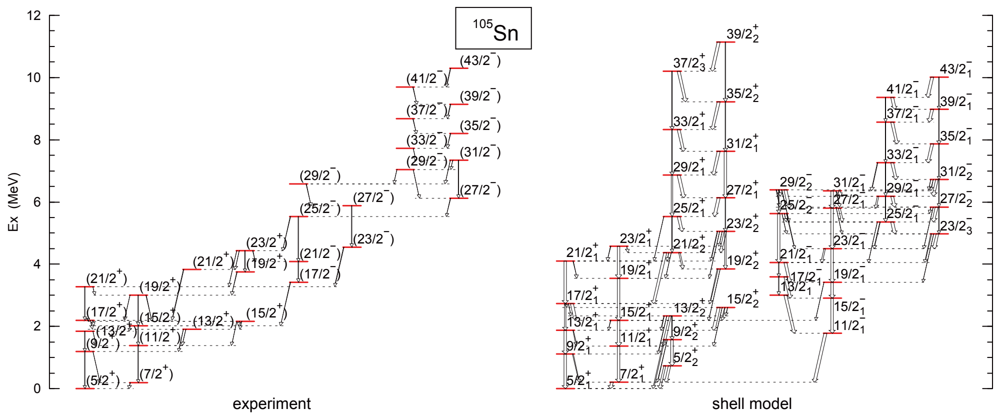

Fig. 1. Energy levels of ^{105}Sn. The experimental data are taken from Refs. 1, 7). The shell-model results are obtained using the code MSHELL64.[8)] The width of the arrow drawn in the shell-model results is proportional to the branching ratio.

*1 Center for Mathematical Sciences, University of Aizu
*2 RIKEN Nishina Center
*3 Department of Physics, University of Tokyo
*4 National Superconducting Cyclotron Laboratory, Michigan State University
*5 Instituut voor Kern- en Stralingsfysica, KU Leuven
*6 Institute of Natural Sciences, Senshu University
*7 Advanced Science Research Center, Japan Atomic Energy Agency
*8 Center for Nuclear Study, University of Tokyo
*9 Department of Physics and Astronomy, Michigan State University
*10 Department of Physics, University of Oslo

References

1) G. de Angelis *et al.*, Nucl. Phys. **654**, 659c (1999).
2) S. Frauendorf, Nucl. Phys. **557**, 259c (1993).
3) M. Honma *et al.*, RIKEN Accel. Prog. Rep. **45**, 35 (2012).
4) M. Honma *at al.*, RIKEN Accel. Prog. Rep. **47**, 64 (2014).
5) M. Hjorth-Jensen *et al.*, Phys. Rep. **261**, 125 (1995).
6) D. R. Entem *et al.*, Phys. Rev. C **68**, 041001(R) (2003).
7) Data extracted using the NNDC WorldWideWeb site from the ENSDF database.
8) T. Mizusaki *et al.*, MSHELL64 code (unpublished).